

A Comparative Analysis Between Various Filters for Three Phase Current Source Inverter

Sameer Khader¹, Abdel-Karim Daud²

¹Palestine Polytechnic University/ Power Electronics Research Unit, Hebron, Palestine
²Palestine Polytechnic University /Department of Electrical Engineering, Hebron, Palestine

ABSTRACT: - This paper investigates three-phase Current Source Inverter (CSI) behaviors energized by battery storage sources replacing Photovoltaic solar system. This source provides energy to a three-phase balanced load throughout passive filters. Various types of filters' configurations are utilized in order to reduce the current and voltage ripples at the inverter output and to reduce the loading stress over the battery bank. Three configurations of filters are investigated C, CLC, and LCL filters with respect to the drawn load current, battery current, and battery loading rate.

A mathematical model for various filters is derived and simulation model using LabVIEW and Multisim platforms were conducted to follow the inverter behaviors when the filters' parameters changed. A comparative analysis between these filters is conducted by changing the filters' capacitance and inductance and following the inverter behaviors. The obtained simulation results stated that LCL filter with Wye connected capacitors presents better performances with respect to output voltage level, loading current, load to battery current utilization ratio at moderate capacitor values comparing with other filters but this advantage disappears at high values of used capacitors due to drawn large battery current.

Index Terms— Current Source Inverter (CSI), Renewable Energy Sources, Photovoltaic Source, PWM, Comparative analysis.

I. INTRODUCTION

Photovoltaic power is considered as one of the most important renewable energy sources [1] in Middle East and used to convert the solar energy into AC signal that is suitable to energize local electrical network with desired voltage and frequency. The photovoltaic system consists of dc source, dc chopper in order to maintain the output dc voltage at values corresponding to the maximum extracted power, dc to ac converter having two main classes voltage source inverter (VSI) and current source inverter (SCI) and output ac filter capable to smooth the output voltage and current to have pure sinusoidal waveform with desired frequency by using both passive and active filters [2], [3]. There are huge numbers of research articles concentrating on voltage source inverters behaviors when being integrated with the solar photovoltaic source and energizing isolated loads of connected to the local network configurations. Meanwhile there are limited research articles describing the behaviors of current source inverter with various ac filters' In the same manner CSI inverters have the advantage rather than VSI when source current is limited such as solar source, or conventional battery source [4]. As well-known pulse width modulation converters (PWM) produce unwanted voltage and current harmonics that is limited by increasing the rate of modulation frequency [5] and proposing optimized design of ac filter. These filters comprise pure C filter, LCL filter and CLC filter combining both CL and LC filter [6]-[9]. The main aim of this paper is to conduct comprehensive comparative study of these filters with respect to obtained output voltage, drawn source current, system efficiency including the filter efficiency and they are of load current to drawn battery current.

II. MATHEMATICAL MODELING

The mathematical modeling and simulation procedure can be divided into the following stages:

- Proposing the three-phase current source inverter circuit;
- Deriving the main mathematical relationships for various filter;
- Simulating the CSI parameters
- Comparison analysis and discussions.

Way out from the proposed electrical circuit shown on Fig.1 with Battery source representing the PV solar source, inverter circuit and filter unit energizing isolated load. The inverter and the filter configurations are

displayed on Fig.2. Sinusoidal PWM modulation technique is applied to generate six pulse combinations needed to turn-on the power switches in predetermined sequence [10].

One of the important key issues in photovoltaic solar sources is the rate of drawn load current to the battery current at various filter's configuration, which in turn investigates the level of temperatures stress on the battery for different values of battery discharging unit.

A. Generating the switching states

The switching states of the describes current source inverter can be expressed by the three binary signals [11], [12] S_a , S_b & S_c according to (1):

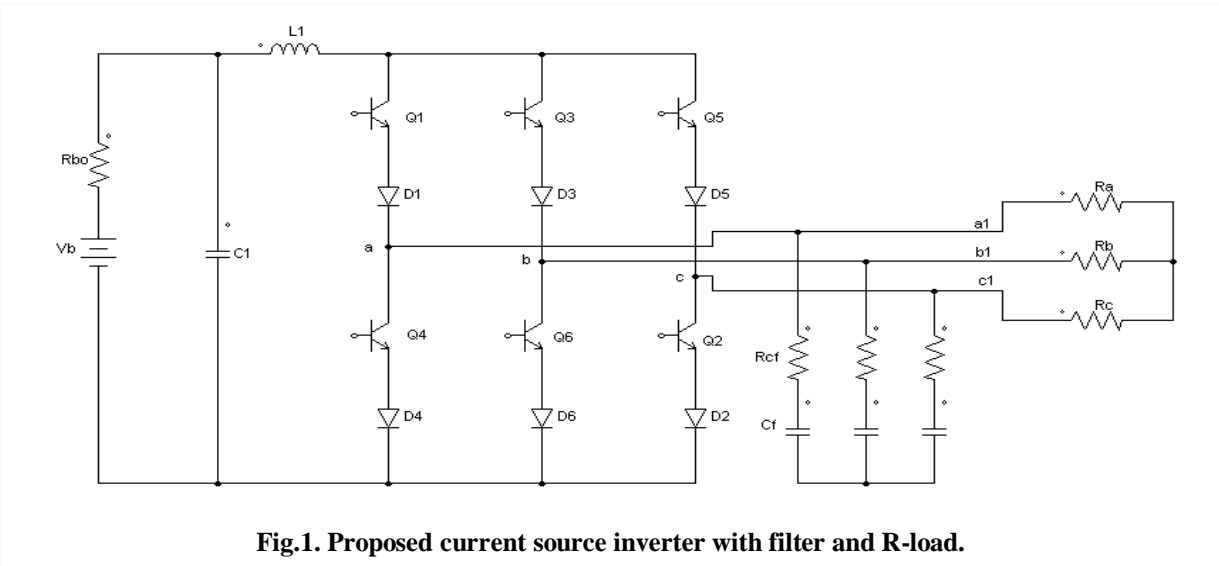
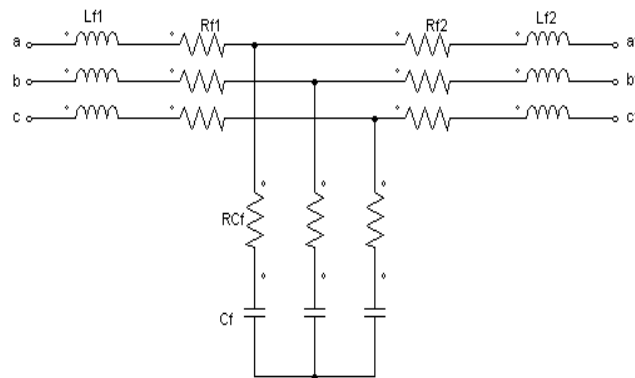


Fig.1. Proposed current source inverter with filter and R-load.

$$\begin{aligned}
 S_a &= \begin{cases} 1, & \text{if } Q1 \text{ ON, and } Q4 = \text{OFF} \\ 0 & \text{if } Q1 \text{ OFF, and } Q4 = \text{ON} \end{cases} \\
 S_b &= \begin{cases} 1, & \text{if } Q3 \text{ ON, and } Q6 = \text{OFF} \\ 0 & \text{if } Q3 \text{ OFF, and } Q6 = \text{ON} \end{cases} \\
 S_c &= \begin{cases} 1, & \text{if } Q5 \text{ ON, and } Q2 = \text{OFF} \\ 0 & \text{if } Q5 \text{ OFF, and } Q2 = \text{ON} \end{cases}
 \end{aligned} \tag{1}$$

According to (1) sinusoidal pulse width modulations (SPWM) signal are generated throughout FPGA module existed in LabVIEW platform [13] as shown on Fig.3, where six variable width pulses are generator required to switch-on three-phase SCI inverter. Sample of these pulses are illustrated on Fig.4 for two switches with complementary operation Q1 and Q4.



a) LCL filter

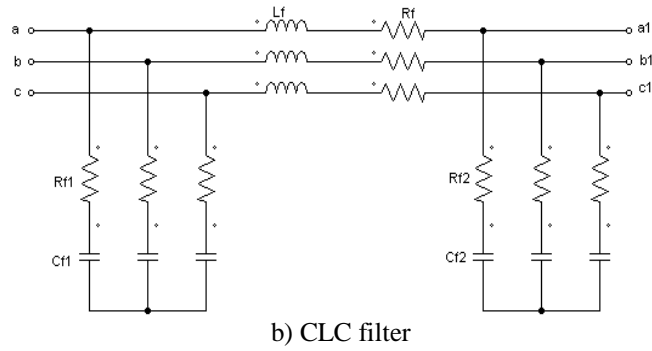


Fig.2. Three phase filters' configuration

According to (1) sinusoidal pulse width modulations (SPWM) signal are generated throughout FPGA module existed in Lab VIEW platform [13] as shown on Fig.3, where six variable width pulses are generator required to switch-on three-phase SCI inverter.

Sample of these pulses are illustrated on Fig.4 for two switches with complementary operation Q1 and Q4.

$$\begin{bmatrix} \dot{I}_{in} \\ \dot{I}_o \\ \dot{V}_C \end{bmatrix} = \begin{bmatrix} a_{11} & a_{12} & a_{13} \\ a_{21} & a_{22} & a_{23} \\ a_{31} & a_{32} & a_{33} \end{bmatrix} \cdot \begin{bmatrix} I_{in} \\ I_o \\ V_C \end{bmatrix} + \begin{bmatrix} b_{11} \\ b_{21} \\ b_{31} \end{bmatrix} \cdot \begin{bmatrix} V_{in} \\ V_o \\ 0 \end{bmatrix} \quad (5)$$

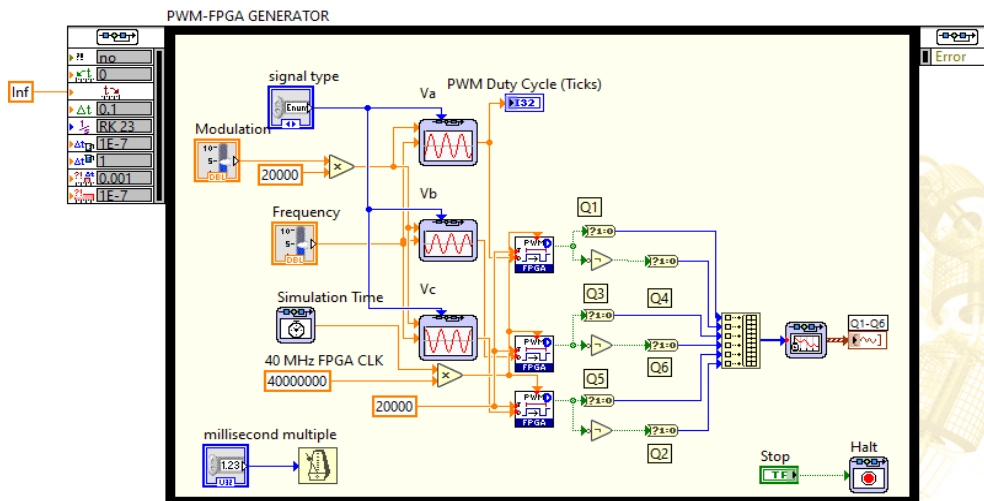


Fig.3. Pulse generator using FPGA.

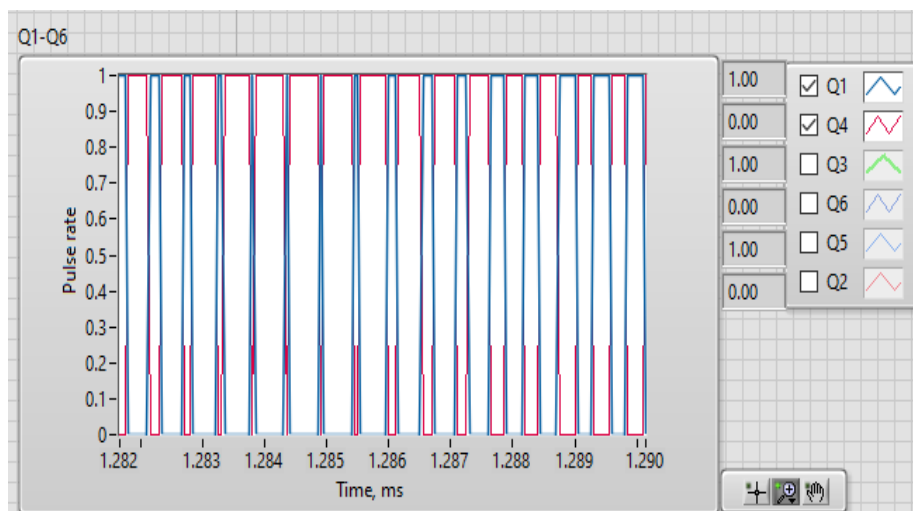


Fig.4. PWM pulses for two switches.

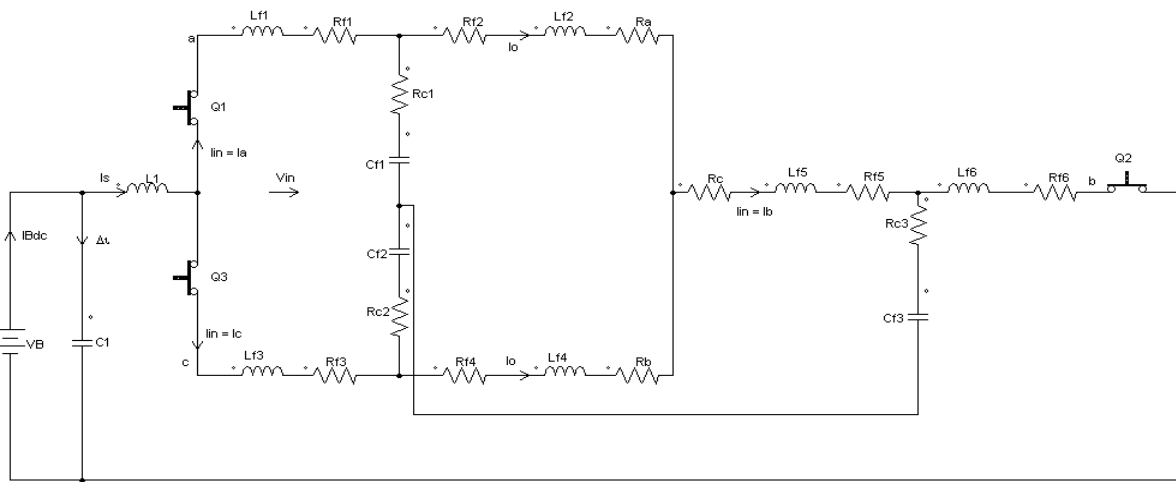


Fig.5. Detailed equivalent circuit of CLC filter for Q1, Q2 & Q3 combination.

Where,

$$\begin{aligned}
 I_{in} &= I_c + I_o \\
 V_o &= I_o R_a \\
 I_c &= C_f \frac{dV_c}{dt} = \frac{1}{C_f} (I_{in} - I_o) \\
 V_{Lf1} &= L_{f1} \frac{dI_{in}}{dt} .
 \end{aligned} \tag{6}$$

The matrix coefficients are displayed in (7), where R_{f1} , R_{f2} and R_c are inductors and capacitor resistances respectively; L_{f1} and L_{f2} are circuit inductances respectively, V_{inv} and V_o are the inverter and load voltage respectively.

$$\begin{aligned}
 a_{11} &= -\frac{R_{f1} + R_c}{L_{f1}}; \quad a_{12} = \frac{R_c}{L_{f1}}; \quad a_{13} = -\frac{1}{L_{f1}} \\
 a_{21} &= -\frac{R_c}{L_{f2}}; \quad a_{22} = -\frac{R_{f2} + R_c}{L_{f2}}; \quad a_{23} = \frac{1}{L_{f2}} \\
 a_{31} &= -\frac{1}{L_{f1}}; \quad a_{32} = +\frac{1}{L_{f2}}; \quad a_{33} = 0; \\
 b_{11} &= \frac{1}{L_{f1}}; \quad b_{21} = -\frac{1}{L_{f2}}; \quad b_{31} = 0.
 \end{aligned} \tag{7}$$

Equation (5) can be expressed as continuous-time state-space variables [14] as stated in (8):

$$\mathbf{X}(k+1) = \mathbf{A}_m \mathbf{X}(k) + \mathbf{B}_m \mathbf{V}(k) \tag{8}$$

where,

$$\mathbf{X}(k+1) = \begin{bmatrix} I_i(k+1) \\ I_o(k+1) \\ V_c(k+1) \end{bmatrix}; \quad \mathbf{X}(k) = \begin{bmatrix} I_i(k) \\ I_o(k) \\ V_c(k) \end{bmatrix};$$

$$\mathbf{A} = \begin{bmatrix} a_{11} & a_{12} & a_{13} \\ a_{21} & a_{22} & a_{23} \\ a_{31} & a_{32} & a_{33} \end{bmatrix}; \quad \mathbf{B} = \begin{bmatrix} b_{11} \\ b_{21} \\ b_{31} \end{bmatrix};$$

$$\mathbf{A}_m = e^{A.Ts}; \quad \mathbf{B}_m = \int_0^{Ts} e^{A.\tau} . B \, d\tau \tag{9}$$

Substituting (9) in (8) yields:

$$\mathbf{X}(k+1) = e^{A.Ts} \mathbf{X}(k) + \int_0^{Ts} e^{A.\tau} . B \, d\tau \mathbf{V}(k). \tag{10}$$

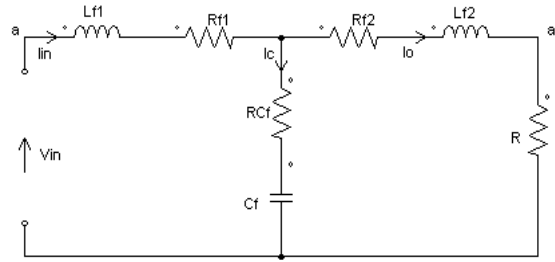


Fig.6. Equivalent circuit of CLC filter.

Now for small sampling time T_s the current change between two adjacent points is negligible, so $I_o(k-1) \cong I_o(k)$ and (8) can be expressed as:

$$I_o(k) = I_{in}(k-1) - \frac{C}{T_s} [V_c(k) - V_c(k-1)] \quad (11)$$

The obtained transfer function between the load current and the inverter current is expressed in (12):

$$G(s) = \frac{I_o(k-1)}{I_{in}(k-1)} = 1 - \frac{C}{T_s} \frac{[V_c(k) - V_c(k-1)]}{I_{in}(k-1)} \quad (12)$$

The capacitor value and charging states for two adjacent points corresponding to the sample time T_s dictate the behavior of this function.

Since the battery storage system plays important role in energy conversion process mainly in isolated generation system and micro-grids [15], [16] the relationship between the load current and battery current is going to be investigated at various filters' configurations.

The balanced inverter current $i_s(\omega t)$ can be composed [17] in two components, DC current component which comes from the battery I_{Bdc} , and high frequency component that depends on the commutation frequency $\Delta i(t)$, which is bypassed through the dc-link capacitor, thus the inverter current can be expressed as:

$$i_s(\omega t) = I_{Bdc} + \Delta i(\omega t) \quad (13)$$

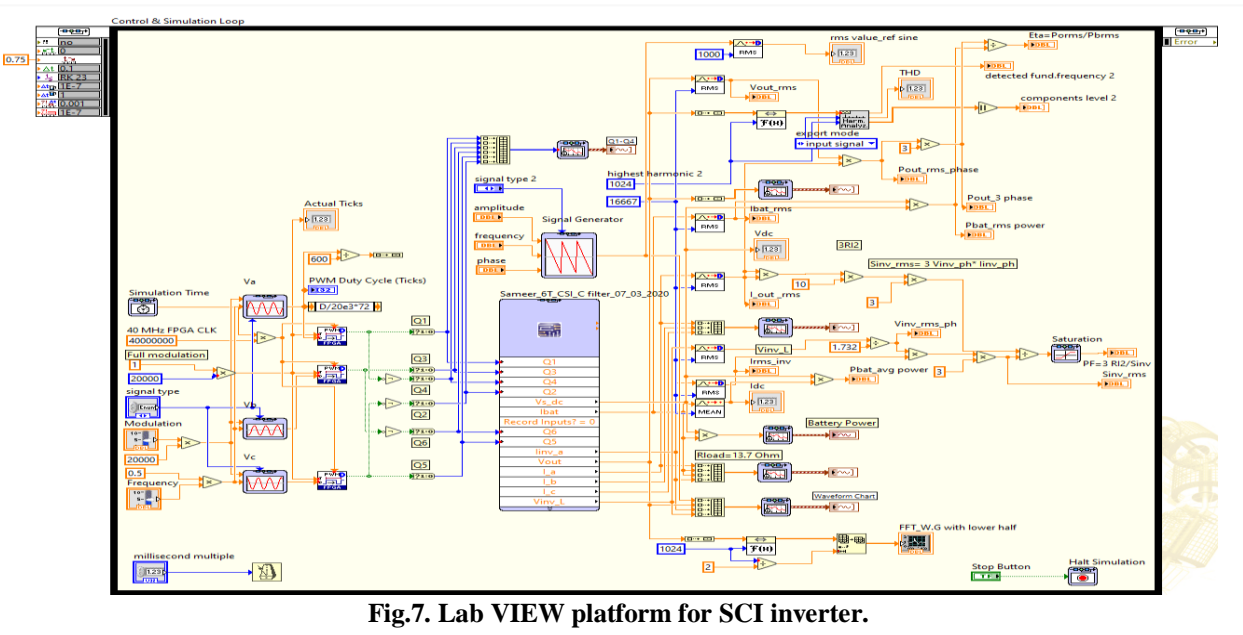


Fig.7. Lab VIEW platform for CSI inverter.

In order to define the value of I_{Bdc} and to estimate the ripples of the inverter current, there is a need to decompose the obtained three phase current in Fourier series using FFT technique [18] yield the following spectrum of current harmonics:

$$\begin{cases} i_a(\omega t) = \sum_{v=0}^{\infty} I_{m_n} \sin(n \cdot \omega t - \theta_n); \\ i_b(\omega t) = \sum_{v=0}^{\infty} I_{m_n} \sin\left(n \cdot \omega t - \frac{2\pi}{3} - \theta_n\right); \\ i_c(\omega t) = \sum_{v=0}^{\infty} I_{m_n} \sin\left(n \cdot \omega t + \frac{2\pi}{3} - \theta_n\right); \\ n = 2 \cdot v + 1. \end{cases} \quad (14)$$

Where I_{m_n} is the magnitude of n-ti harmonic, and θ_n is the phase angle of the same harmonic. Assuming lossless inverter switches and input / output energy balance, the dc input current can be averaged over one period as follows:

$$I_{Bdc} = \frac{3}{2} Ma \cdot \sqrt{\sum_{v=0}^{\infty} (I_{m_n} \cdot \cos \theta_n)^2}; \quad n = 2 \cdot v + 1$$

$$Ma = \frac{Vm_1}{V_{dc}} \quad (15)$$

Where Ma is the modulation index, V_{m_1} is the magnitude of fundamental output phase voltage, V_{dc} is the battery voltage ($V_{dc}=V_B$). For pure sinusoidal harmonic when $n=1$ according to [17], (16) becomes:

$$I_{Bdc} = \frac{3}{2} Ma \cdot I_{m_1} \cdot \cos \theta_1 \quad (16)$$

The input current of each phase can be calculated from switching states (1) and corresponding output current. Consequently, the total inverter input current can be expressed as a sum of three phase current as follow:

$$i_s(\omega t) = Sa \cdot i_a(\omega t) + Sb \cdot i_b(\omega t) + Sc \cdot i_c(\omega t) \quad (17)$$

The current ripples $\Delta i(t)$ for the complete harmonic spectrum can be expressed by combining (16) and (17) yields:

$$\Delta i(\omega t) = i_s(\omega t) - \frac{3}{2} Ma \cdot \sqrt{\sum_{v=0}^{\infty} (I_{m_n} \cdot \cos \theta_n)^2}; \quad (18)$$

These current ripples generate voltage ripples that can be eliminated by proper choice of dc-link capacitor and PWM control strategy, and not scope of this research. In order to investigate the current stress on the battery at various filters' configurations load current to battery current should be determined using the following expression:

$$CRI = \frac{I_{ORMS}}{I_{BRMS}} = \frac{I_{O1}}{\sqrt{\sum_{v=0}^{\infty} I_{on}^2}}; \quad n = 2 \cdot v + 1 \quad (19)$$

where I_{BRMS} is the root mean square of the total battery current that is required to cover fundamental load current I_{O1} and corresponding high order harmonics. These harmonics cause fast battery discharging, excess of heat; and battery life time reduction. The following section simulates the current behaviors at various filters' configuration.

III. SIMULATION RESULTS

The simulation model is built in LabVIEW platform integrated with Multisim platform [19] for various filters' configurations C, CLC & LCL filter which is combination of LC and CL filter. The output voltage, current, effective load power, efficiency, battery current, total harmonic distortion and load to battery current ration are going to be simulated for various filter's capacitance and inductance.

Fig.7 shows the complete LabVIEW program that calls another Multisim program with different filter's configuration, where Fig.8 shows three-phase current source inverter with C-filter.

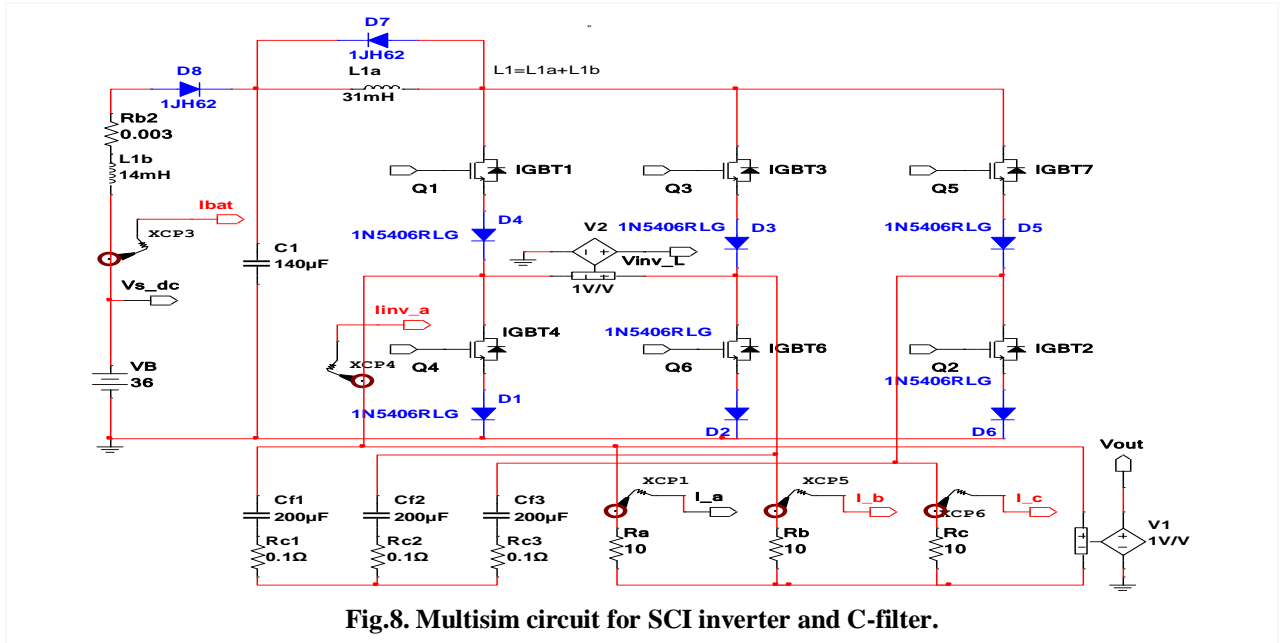


Fig.8. Multisim circuit for SCI inverter and C-filter.

Table I states the values of electrical elements involved in simulation process, while the values of dc-link capacitor and input inductance affect the load and battery current as illustrated in Fig.9, where their values are selected based on optimization procedure for obtaining maximum load current at minimum battery current.

TABLE I: CIRCUIT SPECIFICATIONS

Power elements	$V_B=36V$	$L1=45mH$
		$R_a=10 \Omega$
C-filter	$C_{f1}=200\mu F$	$R_{c1}=0.1 \Omega$
LCL filter*	$C_{f1}=200\mu F$	$R_{c1}=0.1 \Omega$
		$L_{f1}=5\mu H$
CLC filter	$C_{f1}=200\mu F$	$R_{c1}=0.1 \Omega$
		$C_{f2}=200\mu F$

*.-Neglect the values of inductors' resistances R_{f1} and R_{f2} .

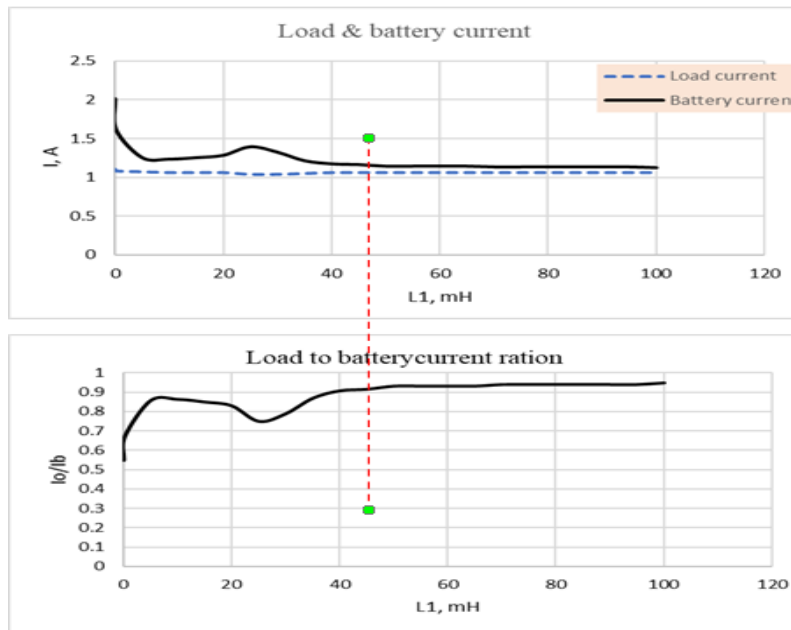
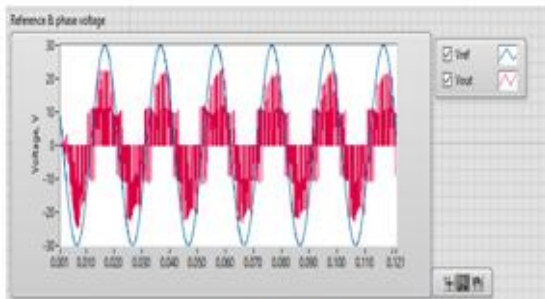


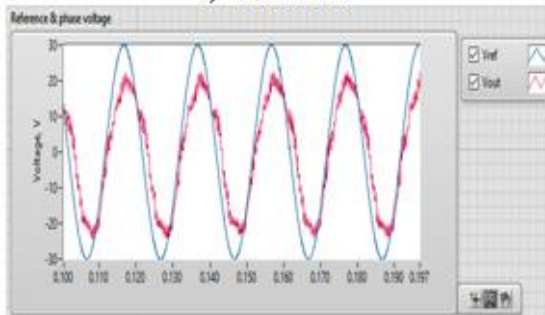
Fig.9. Currents and their ratios versus $L1$.

Having obtained the optimized values of $L1=45\text{mH}$ and $C1=140\mu\text{F}$ and fixing them in further studies, the main parameters are clustered according to the investigated parameters as follow:

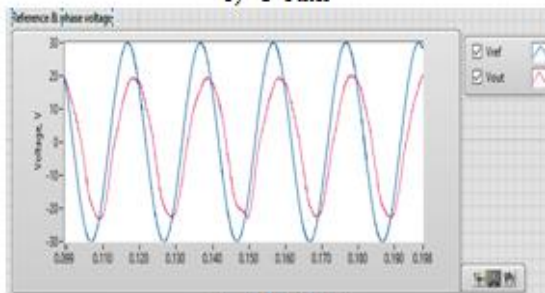
- ✓ Output voltage: the obtained output voltages for various filters are displayed on Fig.10
- ✓ Three-phase current: the obtained three-phase currents are displayed on Fig.11.
- ✓ Battery current; the obtained battery and phase currents are displayed on Fig.12.
- ✓ Battery power: the delivered battery powers are displayed on Fig.13.



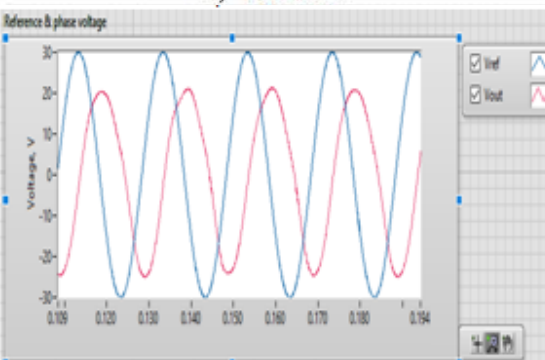
a) Without filter



b) C- Filter

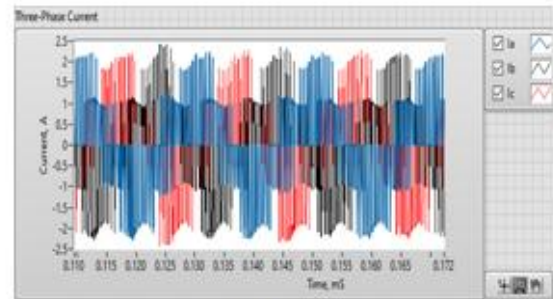


c) LCL- Filter

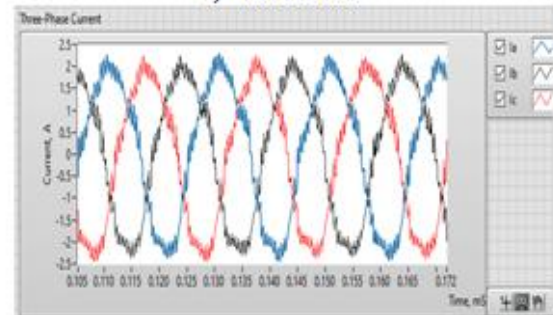


d) CLC- Filter

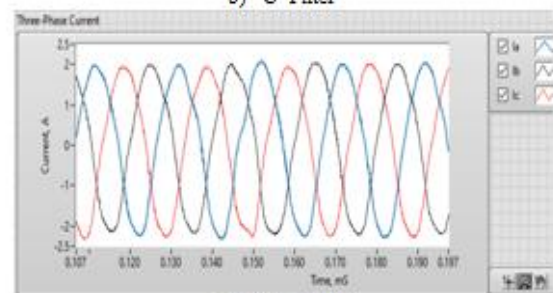
Fig.10. Output and reference voltages for various filters' configurations.



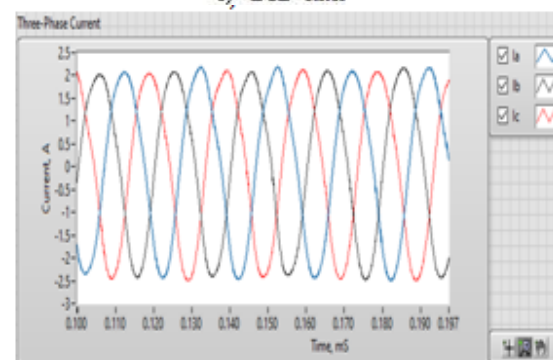
a) Without filter



b) C- Filter



c) LCL- filter



d) CLC- filter

Fig.11. Three-phase current for various filters 'Configurations.

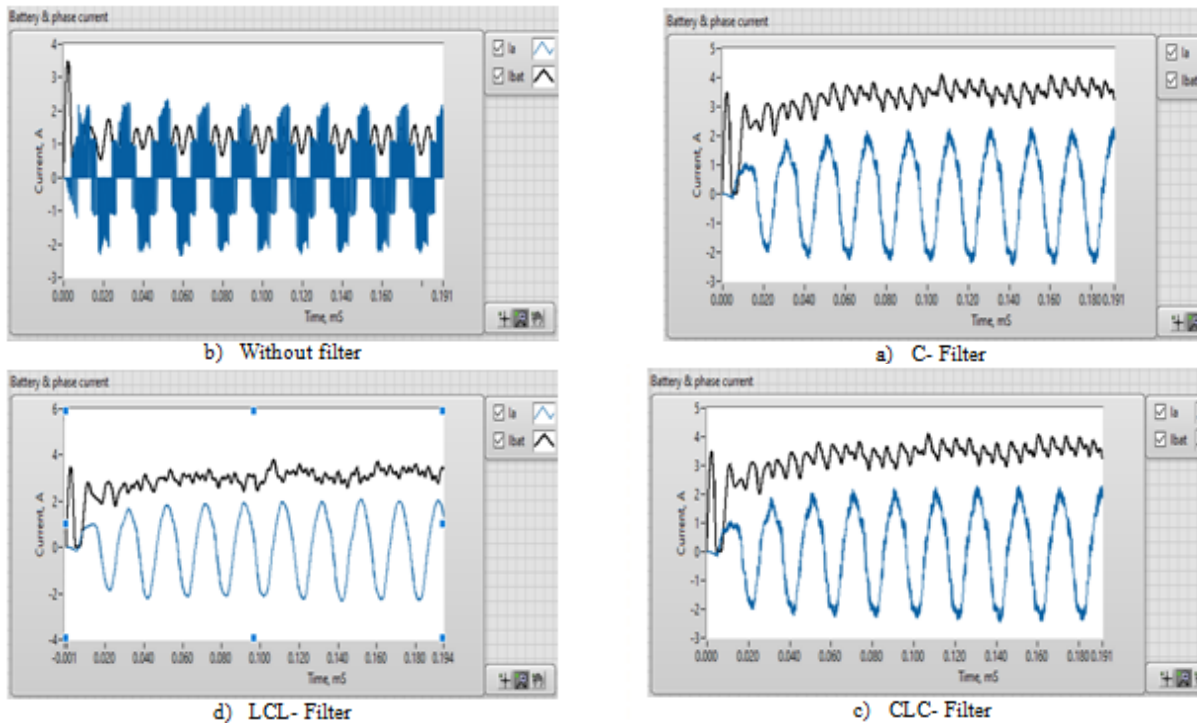


Fig.12. Battery and phase current for various filters' configurations.

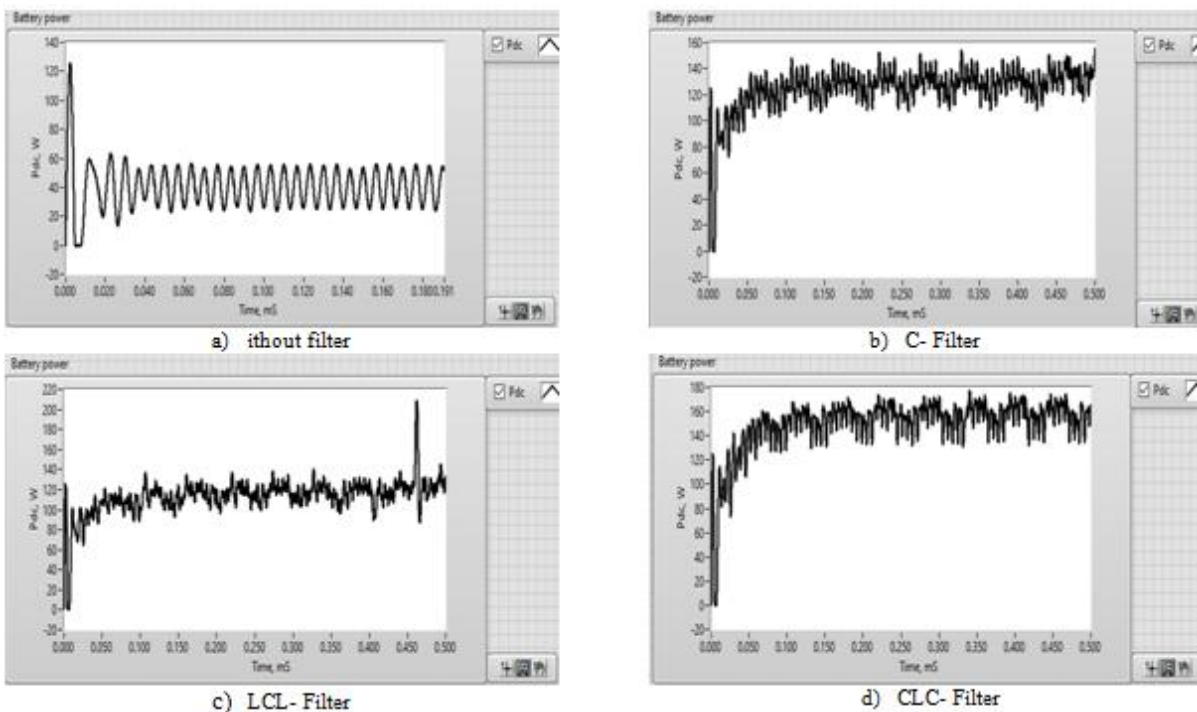


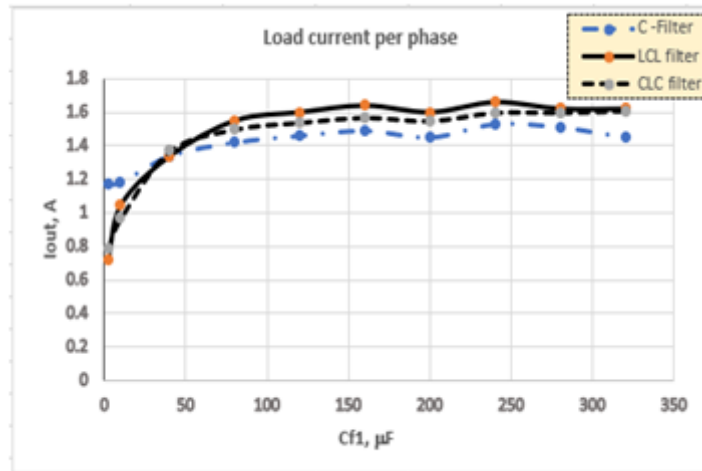
Fig.13. Battery DC power for various filters' configurations.

From these figures it is clearly shown that LCL has less battery consumption, which in turns cause further thermal stress. For detailed comparison, load current, battery current and battery power are going to be investigated for various filter's capacitance and inductance.

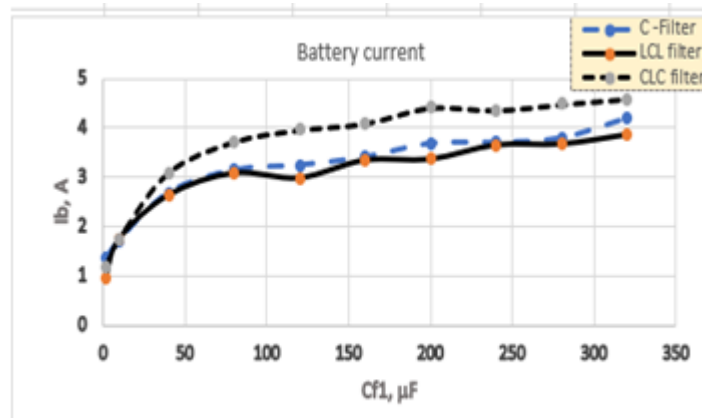
IV. COMPARISON ANALYSIS

After a brief review of the relationships between these parameters over time, it is now the role of assessing the effect of filter's capacitance on these parameters at various filter's configuration as follows:

➤ Fig.14(a) shows the load current at various capacitance where it is shown that CLC filter has dominant values comparing with others causing further increase in the load current with 8.7% at $C_{f1}=120\mu\text{F}$ comparing with C-filter.



a) Load current.



b) Battery current

Fig.14. Battery and load current versus filters capacitance for various filters.

➤ Fig.14(b) shows the battery current for the same conditions as mentioned in previous paragraph, where CLC filter displays better performances with respect to battery current resulting in drop by 8.1% comparing with C-filter and by 22% comparing with CLC filter.

➤ Fig.15 shows the ration between load current and battery current according to (20) with results stated in Table II, where the current ratio difference ΔCRI varies as the capacitor value changes. It is stated that for $C_{f1} \geq 40\mu\text{F}$ CLC filter has dominant role with better CRI.

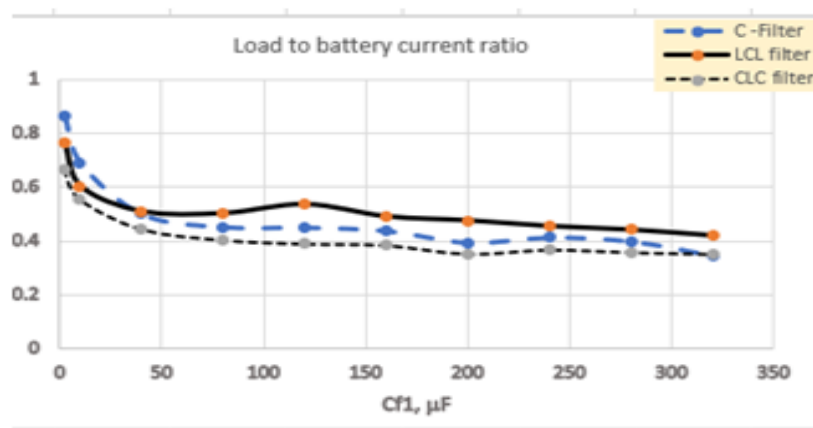
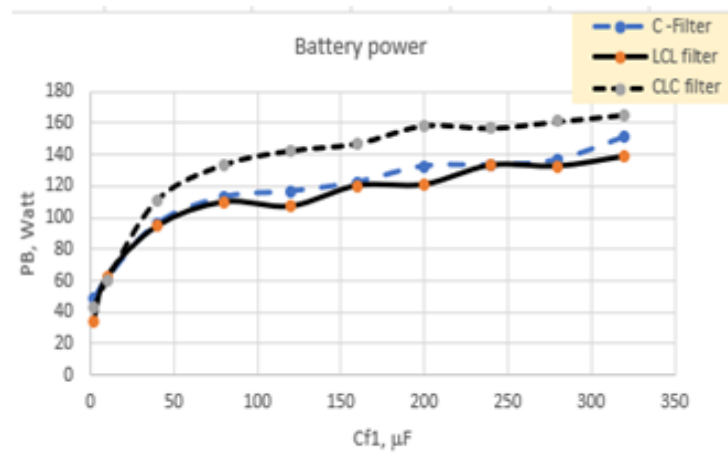


Fig.15. Battery to load current vesus filters capacitance for various filters.

TABLE II: LOAD TO BATTERY CURRENT RATION

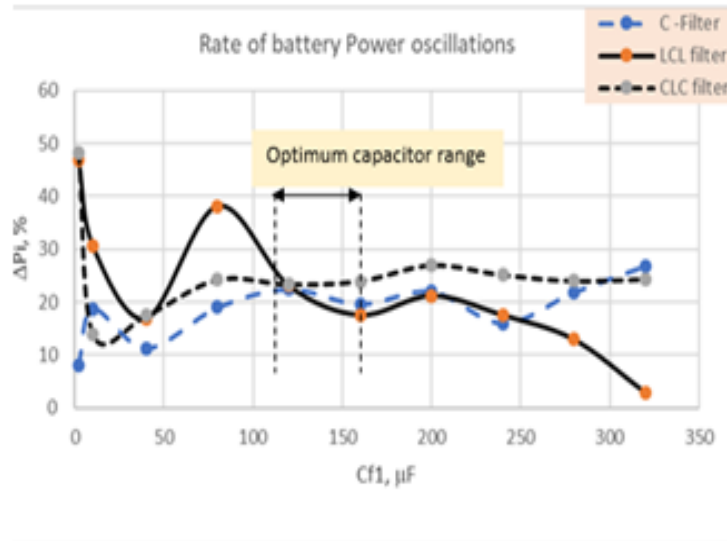
Cf1, μF	C-Filter	LCL filter	CLC filter	ΔCRI %	LCL vs C
2	0.86	0.76	0.66	11.62	↓
10	0.69	0.60	0.55	12.55	↓
40	0.50	0.50	0.44	-1.90	↑
80	0.45	0.50	0.40	-11.28	↑
120	0.45	0.53	0.39	-19.15	↑
160	0.43	0.49	0.38	-12.04	↑
200	0.39	0.47	0.35	-20.85	↑
240	0.41	0.45	0.36	-9.98	↑
280	0.39	0.44	0.35	-10.79	↑
320	0.34	0.42	0.35	-21.27	↑

➤ Fig.16 (a) shows the battery power delivered to the load for various filter’s configuration, where it is shown the delivered power at $C_{f1}=120\mu\text{F}$ is reduced by 8.1% comparing with C filter and by 25% comparing with CLC filter.



a) Battery power.

➤ Fig.16 (b) shows the rate of power oscillation for various filters as stated in (20):



b) Rate of battery power oscillations.

Fig.16. Battery power oscillations for filters capacitance for various filters.

$$\Delta PI\% = \frac{\sqrt{PB_{RMS}^2 - PB_{DC}^2}}{PB_{DC}} * 100 \tag{20}$$

Where PB_{RMS} presents the total delivered power combining the load power and power required to cover the harmonics in form of power oscillations causes excess of heat and battery stress, while PB_{DC} presents the drawn DC power in case of ripple free circuit, where the delivered power is directed to cover the load power.

The difference between these two components presents the power loss and additional heat. From Fig. 16(b) it is shown that LCL filter has less battery power delivered during the capacitance range of $C_{f1} = (115-160) \mu F$ with ΔPI ranging between 23% and 16%. Further increase in capacitance value causes decrease in $\Delta PI\%$ as well causing high battery current to flow.

➤ Fig.17 shows the battery and load current for LCL filter, where it is shown that at $C_{f1} = (110-120) \mu F$ the load current is stabilized at minimum battery current. This mean that further increase of the capacitor value causes only further increase in the battery current resulting an additional stress without significant effect on the load current.

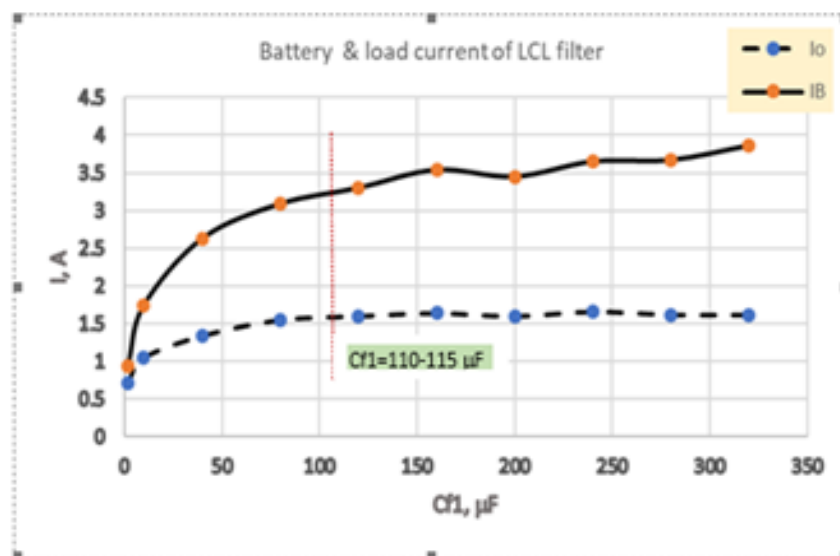


Fig.17. Battery & load current of LCL filter .

V. CONCLUSION & FUTURE WORK

Three phase current source inverter with various filter's configuration of C, LCL and CLC filters are studied, where mathematical model is derived using state-small variables in order to determine the load, inverter phase and battery current.

Then load to battery current ration CRI is derived in order to study the rate of that ratio for various filter's configuration aiming at finding the maximum ration at minimum drawn battery current. In order to determine the rate of battery discharging in form of excess of power needed to cover certain load power a rate of battery power oscillation expression is derived.

Taking into consideration the mentioned procedure, load voltage, load current, battery current, load to battery current ration, and power oscillation performances are studied for different values of capacitor filter C_{fi} where the CLC filter displayed better performances comparing with other in form of:

- An increase of 8.7% in the load current at the same battery current;
- At the same load current CLC filter results a drop in drawn battery current with 8.1% comparing with C filter and 22% comparing with CLC filter;
- LCL filter causes better utilization with respect to load to battery current ratio when the capacitance exceeds 40 μ F;
- The power oscillations reduce by 8.1 % comparing with C filter and 25% comparing with CLC filter which is good indicator for less thermal stress and long discharging time at given load. These values occur when C_{fi} ranging between 110 μ F and 160 μ F, where the load current is stabilized at 110 μ F.

In order to increase CRI to be close to unity, there is a need of realizing feedback control unit based on (13) that realizes effective regulation of inverter current which in turn affects the battery current causing further increase in CRI. This issue could be a task for future work.

REFERENCES

- [1]. Gilbert M. Masters, *Renewable and Efficient Energy Systems*, 1st ed. Wiley, 2004, ch. 9, pp528-565.
- [2]. Misbawu Adami, Shahrouz Ebrahimbanhi, Yue-peng Cheni and Qi-hong Cheni, "Performance of CLC Filters with Shunt APF for Harmonic Current Mitigation", in Proc. 2nd International Conference on Mechatronics, Control and Automation Engineering (MCAE 2017), China, 2017, pp.32-41.
- [3]. Y. Chunyang, L. Tianfa, D. Changwen, Z. Hongwei, X. Jiayang," Study on harmonic current detection method for single-phase PV inverter", In Proc. of China International Conference on Electricity distribution, IEEE, Shenzhen, China, 2014, pp. 1621-1624.
- [4]. H. Haihong, X. Huan, L. Xin, W. Haixin, " The study of active power filters using a universal harmonic detection method", In Proc. of ECCE Asia Downunder, IEEE, Melbourne, VIC, Australia, 2013, pp. 591-595.
- [5]. Muhammad H. Rashid, Narendra Kumar, Ashish Kulkarni, *Power Electronics, Devices, Circuits & Applications*, 4th edition, Pearson, 2014, Ch.6, pp.364-371.
- [6]. F. Bouchafaa, D. Beriber, M.S. Boucherit," Modeling and control of a grid connected PV generation system", In Control & Automation (MED), 18th Mediterranean Conference, Morocco, 2010, pp. 315 – 320.
- [7]. M. Liserre, F. Blaabjerg, S. Hansen, "Design and Control of an LCL-Filter-Based Three-Phase Active Rectifier". In Proc. of the 5th IEEE Conference on Industrial Electronics and Applications (ICIEA'10), Taiwan, 2010, pp. 948–951.
- [8]. Sameer Khader, Abdel-Karim Daud, "Optimization of AC Filter for New Configuration of Single-Phase Current Source PV Inverter Using LabVIEW Platform", WSEAS Transaction on Computer, Vol. 18, pp.187-197, 2019. .
- [9]. Abdel-Karim Daud, Sameer Khader, " A New Design of Single-Phase Current Source PV Inverter with Load Variation Using LabVIEW Platform", International Journal of Innovations in Engineering and Technology (IJJET), Vol.13(2), pp.01-14, 2019.
- [10]. Ayman Y. Yousef, "Space Vector Pulse Width Modulation Technique", International Journal of Emerging Technology in Computer Science & Electronics (IJETCSE), Volume 15 Issue 1, pp.159-165, MAY 2015.
- [11]. Ihab S. Mohamed, Stefano Rosetta, Ton Due Do, Tomislav Tragicize, and Ahmad Zaki Diab," A Neural-Network-based model predictive control of three-phase inverter with an output LC filter", arXiv:1902.09964v3 [cs.SY] 6 Aug 2019.
- [12]. B. Das, "Analysis of Dynamic Performance of Three Phase Induction Motor Using MATLAB Simulation", International Research Journal of Engineering and Technology, Vol. 3, pp 1732-1745, 2016.

- [13]. LabVIEW Simulation Platform, 16 ed., <http://www.ni.com/en-us/shop/labview>.
- [14]. J. G. d. Matos, F. S. F. e. Silva, and L. A. d. S. Ribeiro, "Power Control in AC Isolated Microgrids With Renewable Energy Sources and Energy Storage Systems," *IEEE Trans. Ind. Electron.*, vol. 62, pp. 3490-3498, 2015.
- [15]. Salameh Z. M., M. A. Casacca, and W. A. Lynch, "A mathematical model for lead-acid batteries," *IEEE Trans. Energy Conversion*, 1992, vol.7, pp. 93-98.
- [16]. Marouane, R. and F. Bacha," A maximum-PowerPoint tracking algorithm applied to a photovoltaic water-pumping system", Proceeding of the 8th International Symposium on Advanced Electromechanical Motion Systems and Electric Drives Joint Symposium, July. 1-3, IEEE Xplore Press, Lille, pp.1-6. 2009.
- [17]. Maria Vujacic ID, Manel Hammam ID, Milan Sandvik ID and Gabriele Grand," Analysis of dc-Link Voltage Switching Ripple in Three-Phase PWM Inverters" *Energies* 2018, 11(2), pp.471-485.
- [18]. E. Oran Brigham, "The Fast Fourier Transform and its Applications", E. Avantek, Inc, 1988, pp.167-203.
- [19]. Multisim Simulation Platform, 14.1 ed., <http://www.ni.com/en-us/multisim> 14.1.

CONFLICT OF INTEREST

The authors acknowledge that the work submitted by them is free from any conflict of interest with a third party, and that it is entirely their effort.

AUTHOR CONTRIBUTIONS

First Author: - Derives the mathematical mode, built the simulation model, initialized the simulation data, generated the simulation data and wrote section I, II & III.

Second Author: - Analyzed the obtained results, built various waveforms, optimized several parameters and wrote sections IV & V.

Both authors reviewed the paper and agreed for the obtained results.

Copyright © 2020 by the authors. This is an open access article distributed under the Creative Commons Attribution License ([CC BY-NC-ND 4.0](https://creativecommons.org/licenses/by-nc-nd/4.0/)), which permits use, distribution and reproduction in any medium, provided that the article is properly cited, the use is non-commercial and no modifications or adaptations are made.



Sameer Khader born in Jenin-Palestine in 1962, and received M.Sc. and Ph.D. in Electrical Engineering from Technical University of Sofia, Bulgaria in 1988 and 1993 respectively. His Ph.D. was in the field of Brushless DC Drives and Power Electronics. In 1995, he has been with the Department of Electrical Engineering, Faculty of Engineering, Palestine Polytechnic University, Hebron, Palestine as an Assistant Professor, and since 2014, as a Professor. He spent one sabbatical year at \university of Hartford, CT, USA for the period January-December, 2010. He received Teaching Excellence Award from AMIDEAST, USA, in 2008, and Research Excellence Award in 2009.

Professor Khader, is an IEEE fellowship and member of local and international institutions. He has a lot of publications in the field of power electronics, DC drives, Energy conversion. His present research interests include power electronics converters, renewable energy systems, DC and AC drives.



Abdel-Karim Daud born in Nablus-Palestine in 1958 and received his Master degree in Electrical Engineering from TU Dresden, Germany in 1983 and PhD from TU Berlin in 1990. He was the Director Academic Affairs, Dean of Applied Professions College and several times as Head of electrical engineering department at the Palestine Polytechnic University (PPU), Hebron/Palestine. Since January 2015, he works as Professor in Electrical Engineering Department of PPU. He has published several papers in international journals and conferences. He has a great experience in research projects. His main research interests are electrical machines, electric drives, energy conversion, and renewable energy.